iScience, Volume *23*

Supplemental Information

MutaBind2: Predicting the Impacts of Single and Multiple Mutations on Protein-Protein Interactions

Ning Zhang, Yuting Chen, Haoyu Lu, Feiyang Zhao, Roberto Vera Alvarez, Alexander Goncearenco, Anna R. Panchenko, and Minghui Li

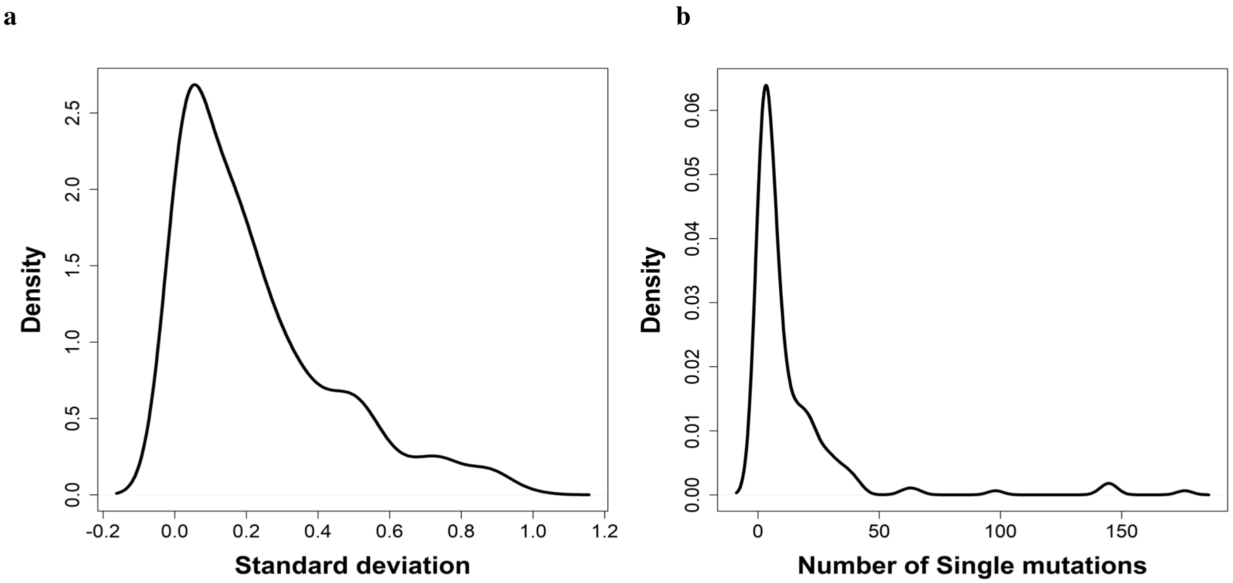

Figure S1. (a) Distribution of the standard deviation for 408 single mutations with multiple experimental measurements of changes in binding affinity in S3310 dataset. (b) Distribution of the number of mutations with $\Delta\Delta G_{exp} > 0$ over protein complexes in S3310 dataset, Related to Figure 1 and Figure 2.

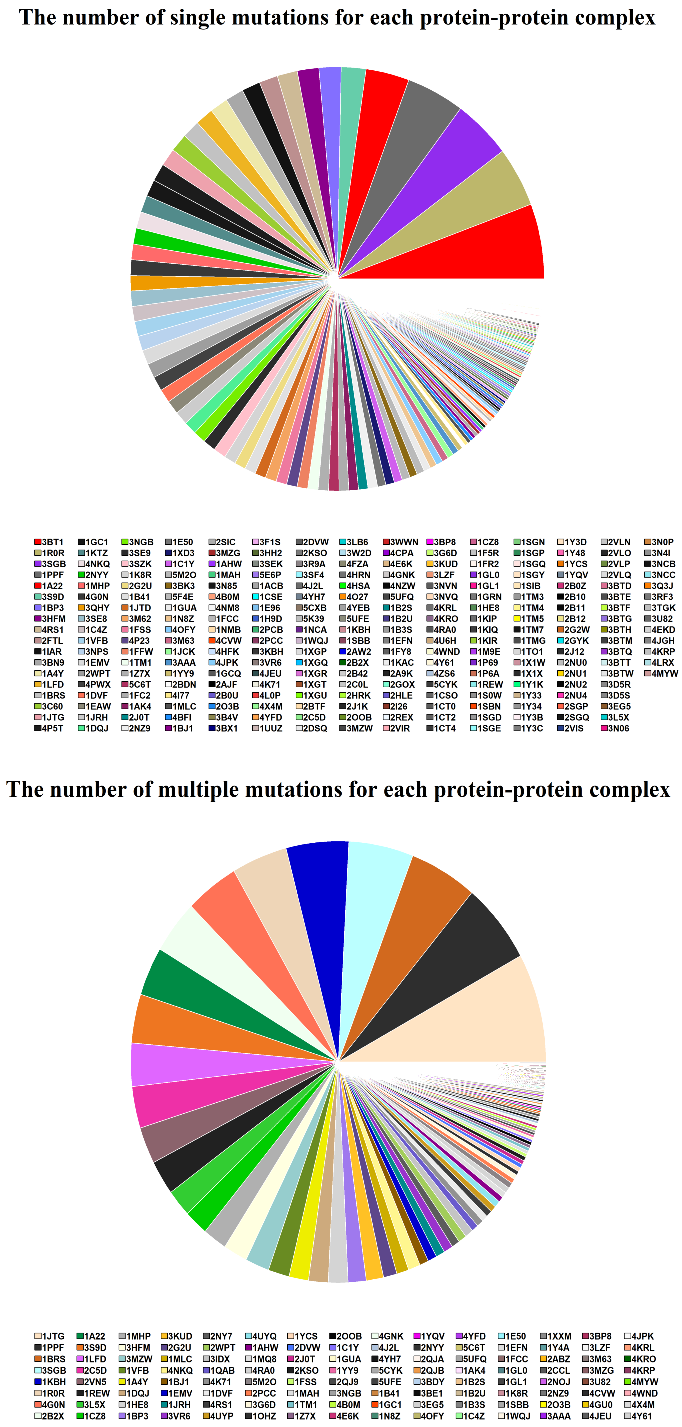

The number of single mutations for each protein-protein complex

The number of multiple mutations for each protein-protein complex

Figure S2. The number of mutations for each protein-protein complex for single and multiple mutation dataset of S3310 and M1337, respectively, Related to Figure 1 and Figure 2.

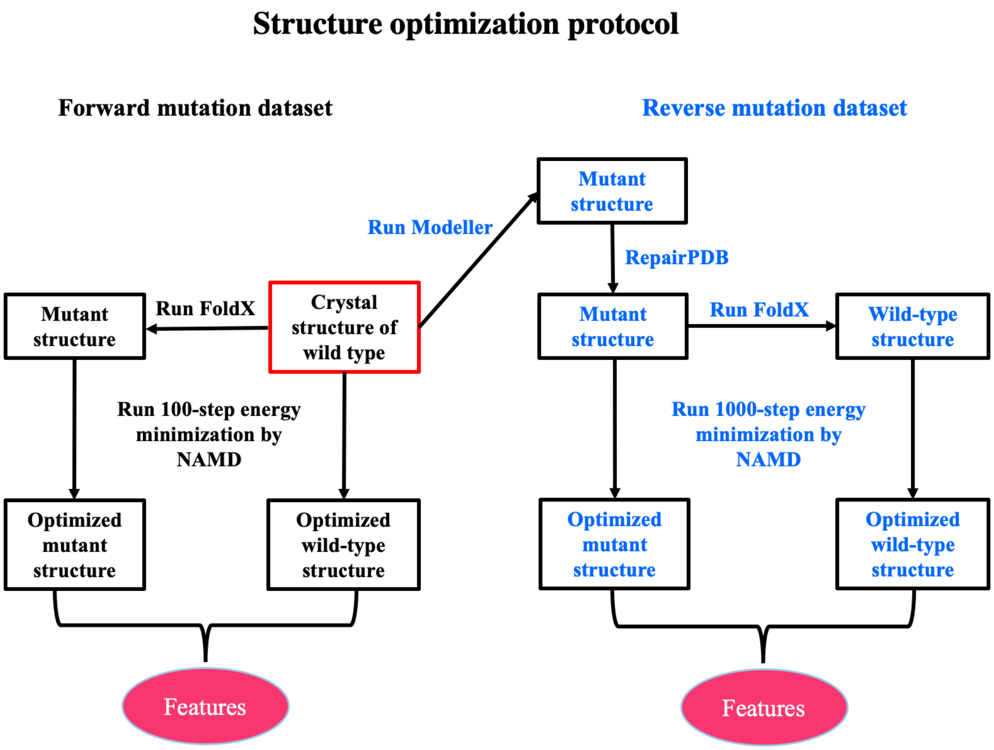
Structure optimization protocol
Forward mutation dataset
Reverse mutation dataset
Mutant structure
Run Modeller
RepairPDB
Mutant structure
Run FoldX
Crystal structure of wild type
Mutant structure
Run FoldX
Wild-type structure
Run 100-step energy minimization by NAMD
Run 1000-step energy minimization by NAMD
Optimized mutant structure
Optimized wild-type structure
Optimized mutant structure
Optimized wild-type structure
Features
Features

Figure S3. The flowchart of the structure optimization protocol, Related to Figure 1 and Figure 2.

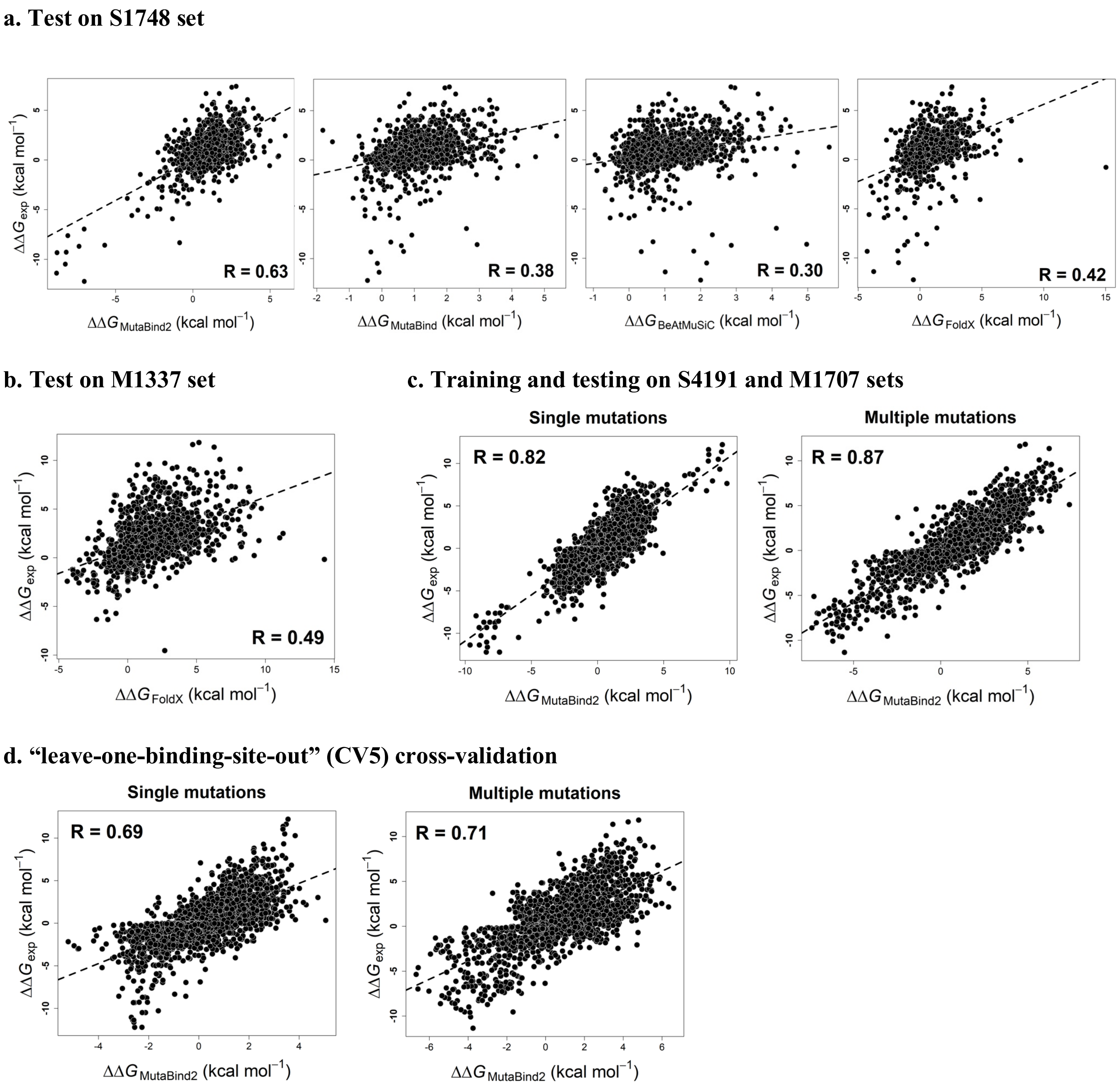

a. Test on S1748 set

b. Test on M1337 set

c. Training and testing on S4191 and M1707 sets

d. “leave-one-binding-site-out” (CV5) cross-validation

Figure S4. Correlation between experimental and calculated changes in binding free energies ($\Delta\Delta G$) for (a) MutaBind2, MutaBind, BeAtMuSiC and FoldX methods tested on S1748 independent dataset. Here MutaBind2 model is trained on the dataset of “Skempi+Reverse”; (b) FoldX tested on M1337; (c) MutaBind2 trained and tested on S4191 and M1707; (d) MutaBind2 tested on S4191 and M1707 using “leave-one-binding-site-out” (CV5) cross-validation respectively, Related to Table 1.

a.

Dataset	Mutations-interaction pairs	Interaction-disruptive mutations	Interaction non-disruptive mutations
Original	4797	903	3894
Mapped to Structure	451(2033)	147(831)	304(1202)

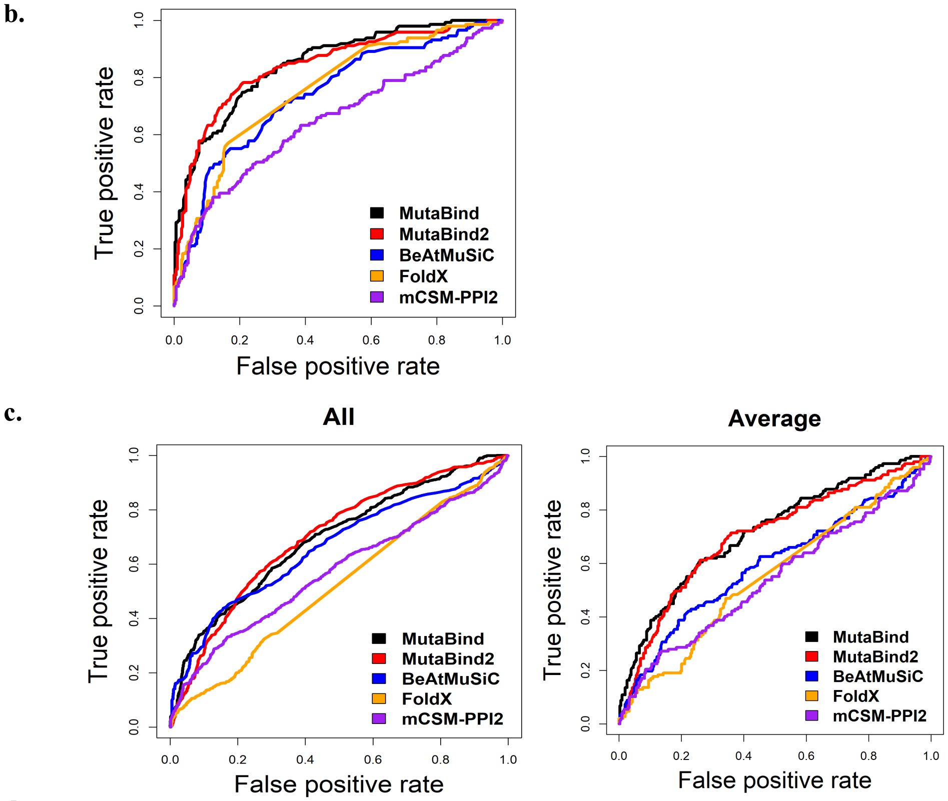

d.

Method	Maximum		All		Average	
	AUC	MCC	AUC	MCC	AUC	MCC
MutaBind2	0.84	0.56	0.70	0.31	0.70	0.34
MutaBind	0.85	0.55	0.69	0.32	0.72	0.34
BeAtMuSiC	0.74*	0.42	0.66*	0.31	0.59*	0.21
FoldX	0.76*	0.42	0.52*	0.10	0.55*	0.12
mCSM-PPI2	0.65*	0.31	0.57*	0.20	0.54*	0.17

Figure S5. Classification performance for predicting of mutations disrupting (decreasing) protein-protein interactions using different methods. (a) The number of mutations used for performance evaluation. “Original”: the impact of 2009 missense mutations across 2185 human protein-protein interactions, interaction profiles for 4797 mutations-interaction pairs were measured by yeast two hybrid (2H) experiments (Fragoza et al., 2019), and 903 mutations were identified as interaction-disruptive mutations. “Mapped to Structure”: the number of mutations/interactions that could be mapped to protein-protein crystal structures. Since one mutation/interaction could be mapped to several PDB structures, the values in parentheses show the total number of mutations/interactions mapped to different PDB structures. (b) ROC curves, the maximum predicted value of binding affinity changes calculated for all mapped PDB structures for each mutation and minimum predicted values were used for interaction non-disruptive mutation. (c) “All”: all predicted values of binding affinity changes calculated using all mapped PDB structures were used for each mutation; “Average”: average values of binding affinity changes calculated using all mapped PDB structures were used for each mutation. (d) AUC and MCC values for classification scenarios using different methods. * denotes a statistically significant difference between MutaBind2 and other methods with p-value < 0.01 estimated by Delong test (DeLong et al.), Related to Figure 3.

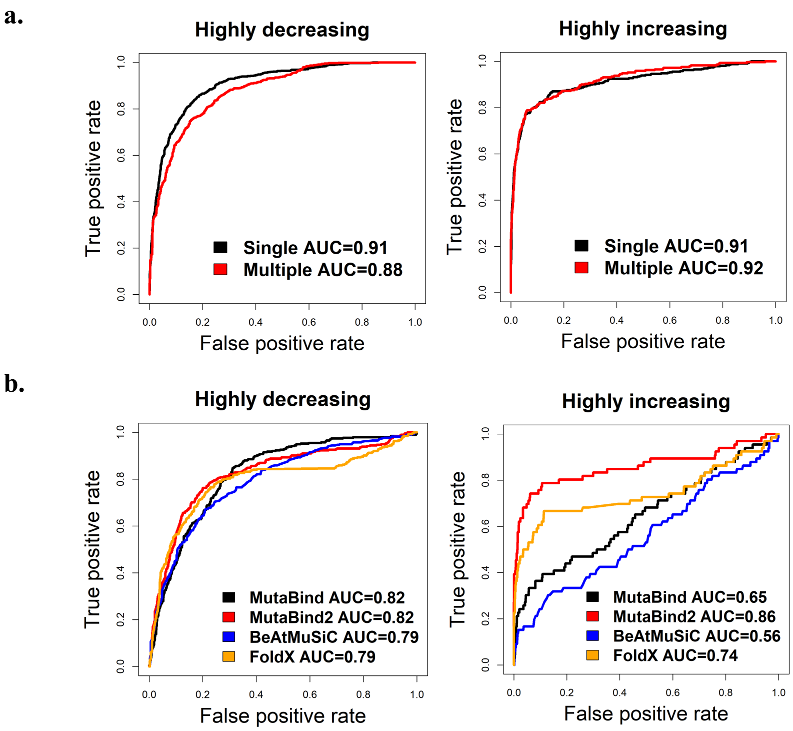

c.

Category		Definition	# of mutations		
			S4191	M1707	S1748
Highly decreasing	Positive	$\Delta\Delta G_{exp}$ (kcal mol^{-1}) >= 1.5	897	690	375
	Negative	$\Delta\Delta G_{exp}$ (kcal mol^{-1}) <= 0.5	2457	810	924
Highly increasing	Positive	$\Delta\Delta G_{exp}$ (kcal mol^{-1}) <= -1.5	425	289	66
	Negative	$\Delta\Delta G_{exp}$ (kcal mol^{-1}) >= -0.5	3289	1233	1599

d.

		True	False
Highly decreasing	Positive	$\Delta\Delta G_{MutaBind2}$≥1.5 & $\Delta\Delta G_{exp}$≥1.5 (TP)	$\Delta\Delta G_{MutaBind2}$≥1.5 & $\Delta\Delta G_{exp}$≤0.5 (FP)
	Negative	$\Delta\Delta G_{MutaBind2}$≤0.5 & $\Delta\Delta G_{exp}$≤0.5 (TN)	$\Delta\Delta G_{MutaBind2}$≤0.5 & $\Delta\Delta G_{exp}$≥1.5 (FN)
Highly increasing	Positive	$\Delta\Delta G_{MutaBind2}$≤-1.5 & $\Delta\Delta G_{exp}$≤-1.5 (TP)	$\Delta\Delta G_{MutaBind2}$≤-1.5 & $\Delta\Delta G_{exp}$≥-0.5 (FP)
	Negative	$\Delta\Delta G_{MutaBind2}$≥-0.5 & $\Delta\Delta G_{exp}$≥-0.5 (TN)	$\Delta\Delta G_{MutaBind}$≥-0.5 & $\Delta\Delta G_{exp}$≤-1.5 (FN)

e.

	Highly decreasing		Highly increasing	
	S4191	M1707	S4191	M1707
Sensitivity	0.83	0.84	0.71	0.75
Specificity	0.95	0.84	0.99	0.97
MCC	0.78	0.68	0.76	0.76
AUC	0.91	0.88	0.91	0.92

Figure S6. (a) ROC curves for predicting mutations highly decreasing and increasing binding affinity using "leave-one-complex-out" cross-validation (CV4) results ($\Delta\Delta G$) of S4191 and M1707, (b) ROC curves for predicting mutations highly decreasing and increasing binding affinity by applying different methods on the independent test set S1748, and (c) Definitions of highly decreasing and increasing mutations and the number of mutations for making ROC curves. True positive rate (Sensitivity) = (TP/TP+FN) and False positive rate = (FP/FP+TN). (d) The definition of true positives (TP), true negatives (TN), false positives (FP) and false negatives (FN) for predicting highly decreasing and increasing mutations. (e) Performance of MutaBind2 for predicting mutations highly decreasing and increasing binding affinity using "leave-one-complex-out" cross-validation (CV4) on S4191, Related to Table 3.

a. Test on 1748 **b. Test on S4191**

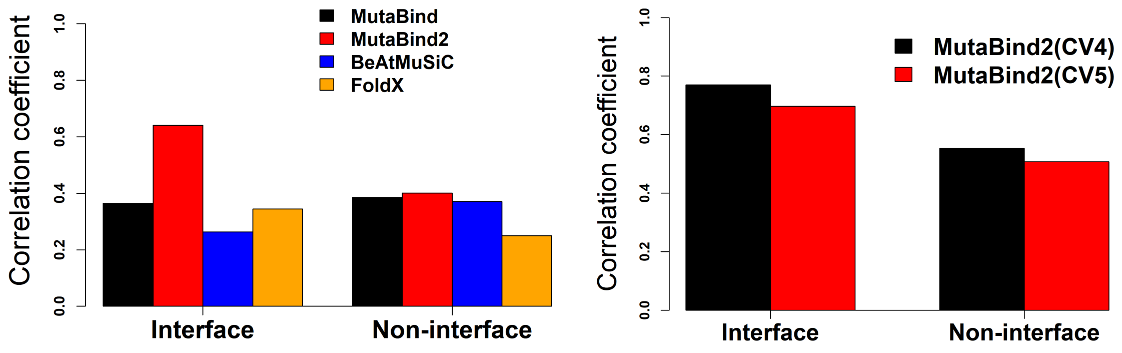

c.

Category	**# of mutations**	
	S1748	**S4191**
Interface	1221	3240
Non-interface	527	951

Figure S7. Pearson correlation coefficients between predicted and experimental ΔΔ*G* for (a) mutations from S1748 test set located on interface and non-interface predicted by different methods. MutaBind2 here is trained on the dataset of "Skempi+Reverse"; (b) mutations from S4191 test set located on interface and non-interface predicted by MutaBind2(CV4) and MutaBind2(CV5). (c) The number of interfacial and non-interfacial mutations for two sets. Only statistically significant correlation coefficients (p-value < 0.01, calculated by one-sample *t*-test) are shown, Related to Table 1 and Figure 2.

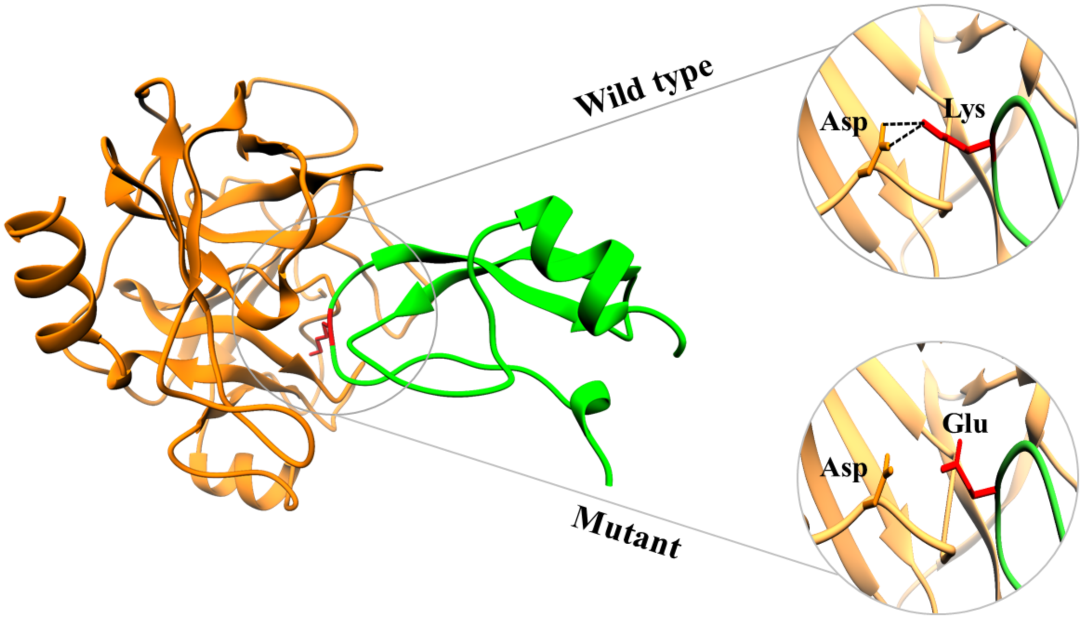

Figure S8. Salt bridges were disrupted after Lys was mutated to Glu in Cationic Trypsin / Pancreatic Trypsin Inhibitor complex (PDB code: 2FTL). The experimental and predicted binding affinity change by MutaBind2 is 9.31 and 9.21 kcal mol^{-1} respectively, Related to Figure 2.

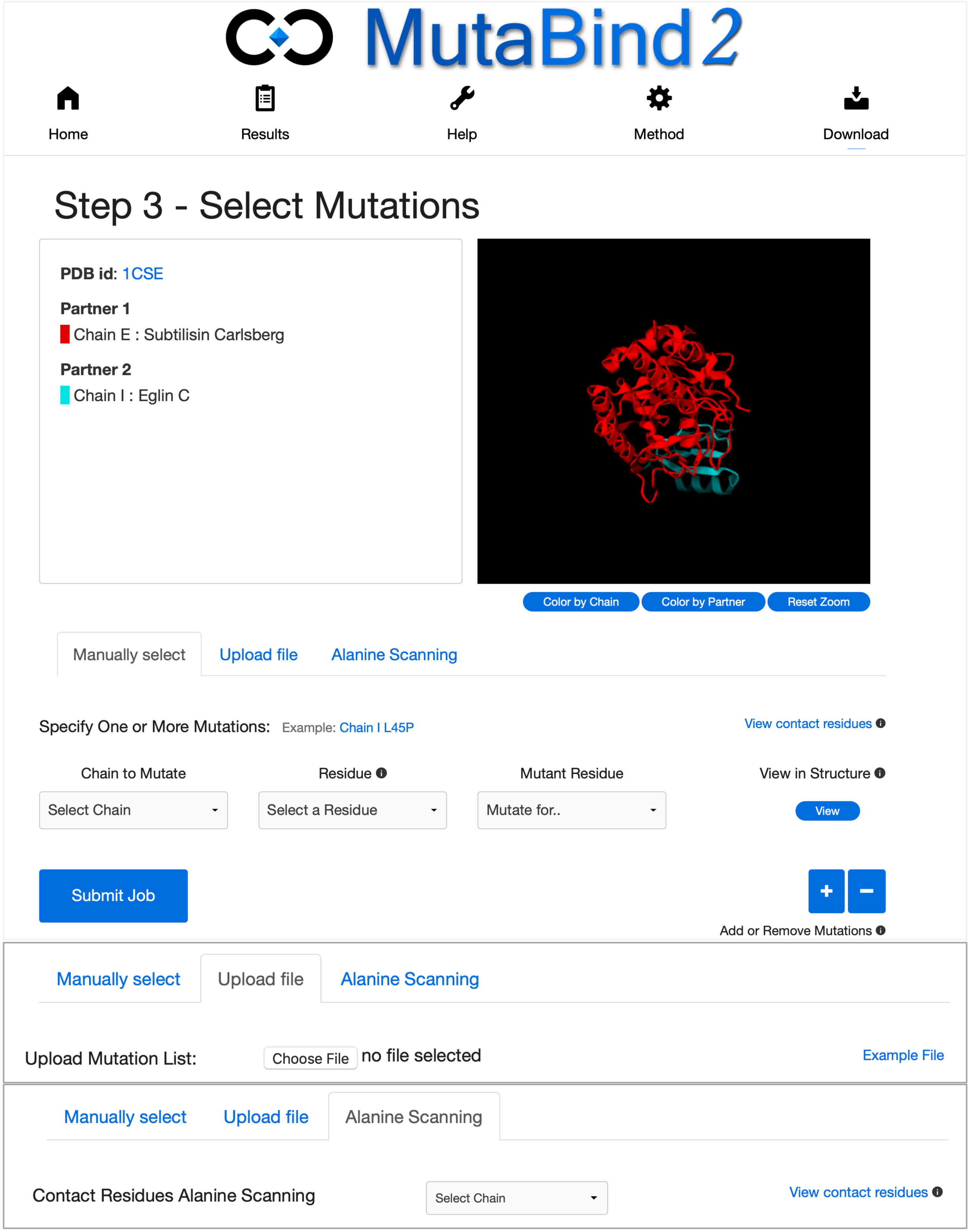

Step 3 - Select Mutations

PDB id: 1CSE

Partner 1

🟥 Chain E : Subtilisin Carlsberg

Partner 2

🟦 Chain I : Eglin C

Specify One or More Mutations: Example: Chain I L45P

Chain to Mutate	Residue	Mutant Residue	View in Structure
Select Chain	Select a Residue	Mutate for..	View

Add or Remove Mutations

Upload Mutation List: Choose File no file selected

Contact Residues Alanine Scanning: Select Chain

Figure S9. The illustration of the third step of mutation selection, Related to Figure 3.

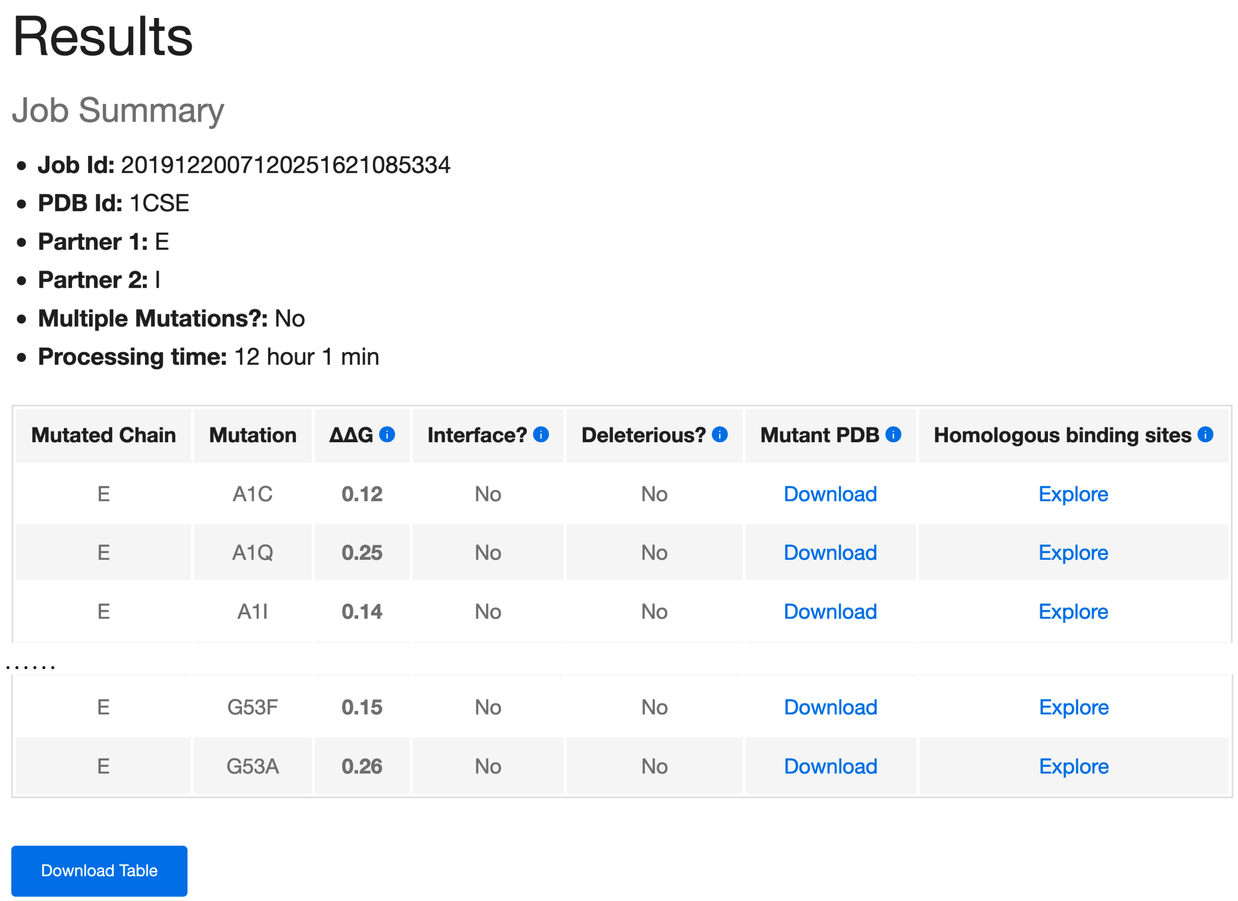

Results

Job Summary

- **Job Id:** 2019122007120251621085334
- **PDB Id:** 1CSE
- **Partner 1:** E
- **Partner 2:** I
- **Multiple Mutations?:** No
- **Processing time:** 12 hour 1 min

Mutated Chain	Mutation	ΔΔG	Interface?	Deleterious?	Mutant PDB	Homologous binding sites
E	A1C	**0.12**	No	No	Download	Explore
E	A1Q	**0.25**	No	No	Download	Explore
E	A1I	**0.14**	No	No	Download	Explore
……						
E	G53F	**0.15**	No	No	Download	Explore
E	G53A	**0.26**	No	No	Download	Explore

Figure S10. Illustration of the time required for MutaBind2 to run predictions for 1000 mutations from a complex with 350 residues, ~12 hours, Related to Figure 3.

a.

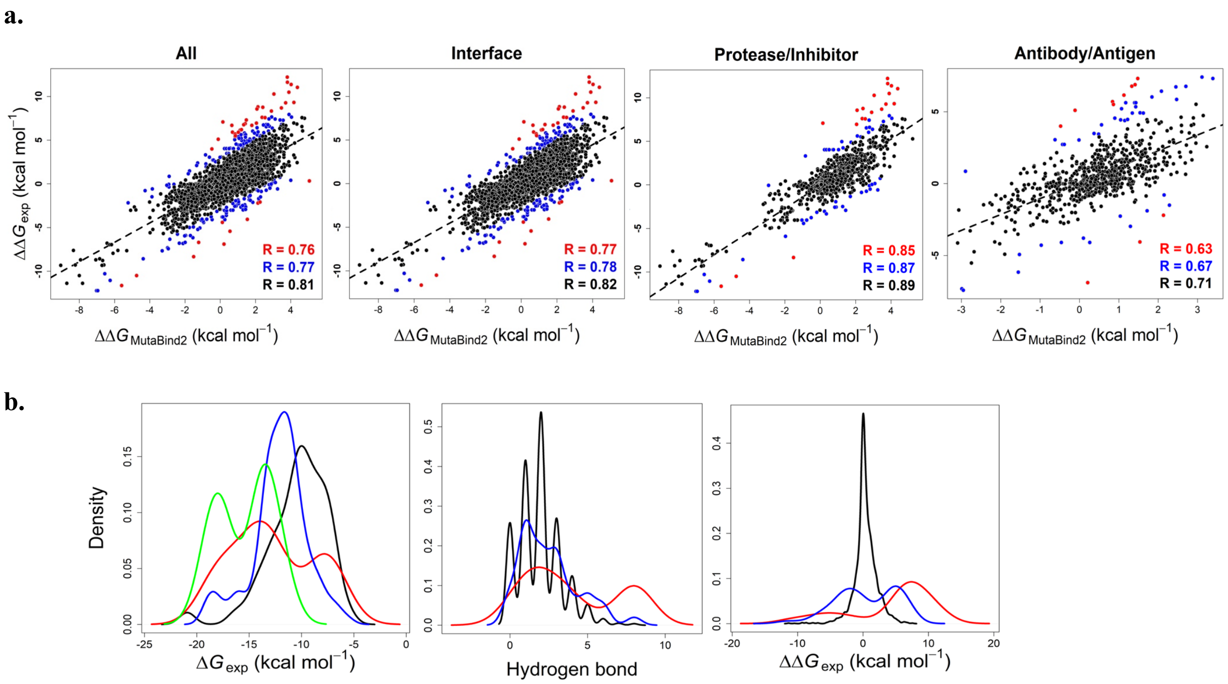

c.

Definition	5% outlier	1% outlier
$(\Delta\Delta G_{MutaBind2}\geq 0$ & $\Delta\Delta G_{exp}\geq 5.0)/\Delta\Delta G_{exp}\geq 5.0$	0.99	0.97
$(\Delta\Delta G_{MutaBind2}<0$ & $\Delta\Delta G_{exp}\leq -5.0/\Delta\Delta G_{exp}\leq -5.0$	0.92	0.67
$(\Delta\Delta G_{MutaBind2}\geq 1.0$ & $\Delta\Delta G_{exp}\geq 5.0)/\Delta\Delta G_{exp}\geq 5.0$	0.88	0.77
$(\Delta\Delta G_{MutaBind2}\leq -1.0$ & $\Delta\Delta G_{exp}\leq -5.0/\Delta\Delta G_{exp}\leq -5.0$	0.92	0.67

d.

PDB id	Mutation	$\Delta\Delta G_{exp}$	MutaBind2 (CV4)
2FTL	K15G	12.22	3.80
2FTL	K15V	11.63	3.81
2FTL	K15D	11.38	4.02
2FTL	K15A	10.29	3.04
2FTL	K15W	8.57	2.08
2FTL	K15I	11.05	4.38
2FTL	K15T	10.49	3.89
2FTL	K15L	8.77	2.41
2FTL	K15Q	9.27	3.71
2FTL	K15M	7.61	2.37
2FTL	K15H	8.69	3.47
2FTL	K15E	9.32	4.18
2FTL	K15F	6.95	2.05
2FTL	V15K	-11.63	-5.60
2FTL	T15K	-10.49	-4.75

e.

Definition		# of mutations	
		Not-Outlier	5% Outlier
Location	Interface	3044	196
	Non-interface	937	14
Type of protein complex	Pr/PI	716	70
	AB/AG	673	51
	AB/AG & Pr/PI	102	5
	TCR/pMHC	148	2
	unknown	2342	82

Pr/PI: protease/inhibitor; AB/AG: antibody/antigen.

Figure S11. Outlier analysis of MutaBind2. The leave-one-complex-out validation (CV4) results of S4191 dataset were used for these analyses. (a) Experimental and predicted values of changes in binding affinity for all single mutations, mutations on protein-protein binding interfaces, mutations from protease/inhibitor and antibody/antigen complexes, respectively. Black: all mutations except for outliers; blue: 5% outliers; red: 1% outliers. (b) Distibution of experimental binding affinity for wild-type complexes (ΔG_{exp}), the number of hydrogen bonds formed by mutated

sites (Hydrogen bond) and experimental binding affinity changes upon mutations ($\Delta\Delta G_{exp}$), respectively. Black: all mutations with the exception of outliers; blue: 5% outliers; red: 1% outliers; green: mutations from seven complexes (PDB ID: 2FTL, 3HFM, 1PPF, 1BRS, 3QHY, 1DQJ and 1B41) in the 5% outlier, and the reason for showing these seven complexes is that they have more mutations (more than five mutations) included in the 5% outlier. (c) True positive rate (d) Mutations from a complex of bovine pancreatic trypsin inhibitor and bovine β-trypsin included in 1% outlier. (e) The number of mutations in categories of interface, non-interface and different types of protein complexes, Related to Figure 2.

Table S1. Experimental datasets used for training and testing different methods, Related to Figure 1, Figure 2, Table 1, Table 2 and Table 3.

Dataset	**Description**
Single mutations	
S3310	Compiled from SKEMPI2
S4191	S3310 plus reverse mutations; **training dataset of MutaBind2, single mutation model**
S4169	Compiled from SKEMPI2
S8338	S4169 plus all reverse mutations**; training dataset of mCSM-PPI2**
Skempi	1925 mutations extracted from SKEMPI; training dataset of MutaBind
S1748	Mutations included in S3310 but not in Skempi
S877	Mutations contained in S4169 but not in S3310
S487	Compiled by iSEE including 487 mutations contained in SKEMPI2 but not in SKEMPI
S33	33 mutations of MDM2-P53 complex (PDB 1YCR) that are not included in SKEMPI2
S19	19 mutations from INTERLEUKIN-4 / RECEPTOR ALPHA CHAIN COMPLEX (PDB 1IAR) that are not included in SKEMPI2
Multiple mutations	
M1337	Compiled from SKEMPI2
M1707	M1337 plus reverse mutations; **training dataset of MutaBind2 multiple mutation model**

S33, S19 and S487 datasets were obtained from https://github.com/haddocking/iSee. Protein complexes with more than 10 single mutations with experimental values of binding affinity changes from "Skempi" were used to build its reverse mutation set.

Dataset	**All mutations**		$\Delta\Delta G_{exp} > 0$		$\Delta\Delta G_{exp} < 0$	
	# of mutations	**# of complexes**	**# of mutations**	**# of complexes**	**# of mutations**	**# of complexes**
S3310	3310	265	2504	188	712	173
S3310.R	881	49	0	0	881	49
S4191	4191	265	2504	188	1593	188
M1337	1337	120	1059	100	272	64
M1337.R	370	19	0	0	370	19
M1707	1707	120	1059	100	642	72
S4169	4169	319	3126	238	901	203
Skempi	1925	80	1478	77	410	43
S1748	1748	212	1286	137	390	145
S877	877	63	643	56	186	34
S487	487	65	414	55	66	33
S33	33	1	27	1	6	1
S19	19	1	15	1	3	1

S3310.R: reverse mutations dataset of S3310; M1337.R: reverse mutations dataset of M1337.

Table S2. The importance of each feature for MutaBind2 single and multiple mutation models, respectively. IncNodePurity is used for describing the importance which is the total decrease in node impurities from splitting on the variable, averaged over all trees, Related to Figure 1, Figure 2, Table 1, Table 2 and Table 3.

Model	**Feature**	**Importance**
Single	$\Delta\Delta E_{vdw}$	1605
	$\Delta\Delta G_{solv}$	2523
	$\Delta\Delta G_{fold}$	3027
	SA_{com}^{wt}	1522
	SA_{part}^{wt}	1577
	CS	4555
	N_{cont}^{wt}	2032
Multiple	$\Delta\Delta E_{vdw}$	1894
	$\Delta\Delta G_{solv}$	1984
	$\Delta\Delta G_{fold}$	3784
	SA_{com}^{wt}	1614
	SA_{part}^{wt}	1226
	CS	3852
	ΔE_{vdw}^{wt}	2313

Table S3. MutaBind2 performance, Related to Table 1.

Model	**Training/Test set**	**All mutations**			$\Delta\Delta G_{exp} \geq 0$		$\Delta\Delta G_{exp} < 0$	
		R	**RMSE**	**Slope**	**R**	**RMSE**	**R**	**RMSE**
Single	S4191/S4191	0.82	1.19	1.09	0.72	1.13	0.72	1.28
	S4191/S3310	0.76	1.16	1.07	0.72	1.13	0.74	1.25
	S4191/S3310.R	0.69	1.30	0.89	-	-	0.69	1.30
Multiple	M1707/M1707	0.87	1.61	1.14	0.73	1.54	0.75	1.72
	M1707/M1337	0.78	1.56	1.14	0.73	1.54	0.44	1.64
	M1707/M1337.R	0.75	1.78	1.01	-	-	0.75	1.78

R: Pearson correlation coefficient between experimental and predicted *ΔΔG* values. RMSE (kcal mol^{-1}): root-mean square error, is the standard deviation of the residuals (prediction errors). Slope: the slope of the regression line between experimental and predicted ΔΔG values. All reported correlation coefficients are statistically significantly different from zero (p-value << 0.01).

Table S4. The performance for Random Forest regression (RF), Support Vector Machine (SVM) and eXtreme Gradient Boosting (XGBoost) methods on single mutation training dataset S4191. CV4: leave-one-complex-out validation; CV5: leave-one-binding site-out validation, Related to Table 1 and Figure 2.

Method	**Validation**	**All mutations**		$\Delta\Delta G_{exp} \geq 0$		$\Delta\Delta G_{exp} < 0$	
		R	**RMSE**	**R**	**RMSE**	**R**	**RMSE**
RF	CV4	0.76	1.34	0.61	1.31	0.67	1.39
	CV5	0.69	1.50	0.54	1.41	0.47	1.65
SVM	CV4	0.72*	1.42	0.55*	1.41	0.66	1.43
	CV5	0.61*	1.62	0.45*	1.54	0.41*	1.74
XGBoost	CV4	0.75*	1.35	0.58*	1.34	0.70*	1.35
	CV5	0.67*	1.53	0.50*	1.45	0.46	1.66

*p-value < 0.01 compared to Random Forest (Hittner2003 test)

Table S5. Comparison of methods' performance for mutations from two independent test sets S33 and S19, Related to Table 2.

Methods	**R**	**RMSE**
S33, 33 mutations		
MutaBind2	0.59	1.07
MutaBind	0.59	1.18
iSEE	0.62	0.81
mCSM-PPI2	0.75*	0.63
BeAtMuSiC	0.48	1.02
FoldX	0.50	1.36
S19, 19 mutations		
MutaBind2	0.65	1.33
MutaBind	0.67	1.27
iSEE	0.73	1.37
mCSM-PPI2	0.41[a]	1.61
BeAtMuSiC	0.24[b]*	1.70
FoldX	0.72	1.15

All presented values of correlation coefficients are statistically significantly different from zero (p-value < 0.01) except for [a]p-value = 0.08 and [b] p-value = 0.32. * show statistically significant difference with p-value < 0.05 compared to MutaBind2 (Hittner2003 test implemented in R package *cocor* is used for comparing correlation coefficients (Diedenhofen and Musch, 2015; Hittner et al., 2003)). The majority mutations in S33 and S19 are mutations decreasing binding affinity with experimentally measured $\Delta\Delta G_{exp}$ ≥ -0.38 and -0.24 kcal mol^{-1}, respectively.

Table S6. Comparison of performance between MutaBind2 and mCSM-PPI2, Related to Table 2.

Training/Test	**Methods**	**All mutations**			$\Delta\Delta G_{exp} \geq 0$		$\Delta\Delta G_{exp} < 0$	
		R	**RMSE**	**Slope**	**R**	**RMSE**	**R**	**RMSE**
S4191/S3310	MutaBind2	0.76	1.16	1.07	0.72	1.13	0.74	1.25
S4169/S3310	mCSM-PPI2	0.76	1.20	1.29	0.69**	1.20	0.62**	1.17
S4169/S4169	MutaBind2	0.74	1.18	1.13	0.73	1.10	0.62	1.43
	mCSM-PPI2	0.76*	1.19	1.29	0.69**	1.20	0.56*	1.17
S8338/S8338	MutaBind2 CV4	0.74	1.37	1.08	0.64	1.33	0.58	1.41
	MutaBind2 CV5	0.66	1.53	1.17	0.54	1.47	0.43	1.60
	mCSM-PPI2 CV4	0.75	1.30	*NA*	*NA*	*NA*	*NA*	*NA*
	mCSM-PPI2 CV5	0.67	1.39	*NA*	*NA*	*NA*	*NA*	*NA*

**p-value < 0.01 and *p-value < 0.05 compared to MutaBind2 (Hittner2003 test). NA: Data not available. The $\Delta\Delta G$ values for mCSM-PPI2 trained and tested on S4169 (forward mutation dataset for parameterizing mCSM-PPI2 method) were obtained from http://biosig.unimelb.edu.au/mcsm ppi2/. $\Delta\Delta G$ values for mCSM-PPI2 trained and tested on S8338 (training dataset of mCSM-PPI2 method) were not provided on mCSM-PPI2 website, and the R and RMSE values for CV4 and CV5 were obtained from paper (Rodrigues et al., 2019).

S4191/S3310: MutaBind2 trained on S4191 and tested on S3310.

S4169/S4169: MutaBind2 retrained on S4169 and tested on S4169.

S8338/S8338: CV4 and CV5 validation for MutaBind2 retrained on S8338 and tested on S8338.

Table S7. Performance of MutaBind2 parameterized on different datasets where the reverse mutation dataset was compiled using complexes with a different number of mutations binned from 5 to 100. Related to Table 1 and Table 2.

a. Performance of MutaBind2 retrained on "S3310+Reverse" set and tested on independent datasets of S487 and S877.

Cutoff	**All mutations**		**$\Delta\Delta G_{exp} > 0$**		**$\Delta\Delta G_{exp} < 0$**	
	# of mutations	**# of complexes**	**# of mutations**	**# of complexes**	**# of mutations**	**# of complexes**
S3310	3310	265	2504	188	712	173
5 to 30	4458	265	2504	188	1860	211
10 to 30	4191	265	2504	188	1593	188
15 to 30	4023	265	2504	188	1425	184
10 to 50	4517	265	2504	188	1919	188
10 to 100	4741	265	2504	188	2143	188
All	6620	265	3216	265	3216	265

Protein-protein complexes in S3310 with the number of $\Delta\Delta G_{exp}$ > 0 mutations binned from 5 to 30, 10 to 30, 15 to 30, 10 to 50 and 10 to 100 were used for building the reverse mutation dataset. All: with every single forward mutation in S3310 being reversed. (The distribution of the number of $\Delta\Delta \mathrm{G}_{\mathrm{exp}} > 0$ mutations over protein complexes is shown in Figure S1b).

Dataset	**Cutoff**	**R**	**RMSE**
S487	**10 to 30**	**0.41**	**1.25**
	5 to 30	0.39**	1.28
	15 to 30	0.42*	1.23
	10 to 50	0.41	1.26
	10 to 100	0.40	1.26
	All	0.36**	1.31
S877	**10 to 30**	**0.55**	**1.37**
	5 to 30	0.54*	1.38
	15 to 30	0.55	1.37
	10 to 50	0.55	1.37
	10 to 100	0.54	1.38
	All	0.53**	1.40

* show statistically significant difference with p-value < 0.05 and **p-value < 0.01 compared to MutaBind2 trained on S4191 set where reverse mutation dataset was compiled using the cutoff of "10 to 30". For testing on S487 set, MutaBind2 was retrained after removing S487 from the training dataset.

b. Performance of MutaBind2 retrained on "Skempi+Reverse" set and tested on the independent dataset of S1748.

Cutoff	**All mutations**		**$\Delta\Delta G_{exp} \geq 0$**		**$\Delta\Delta G_{exp} < 0$**	
	R	**RMSE**	**R**	**RMSE**	**R**	**RMSE**
10 to 30	**0.63**	**1.25**	**0.45**	**1.17**	**0.77**	**1.52**
5 to 30	0.62*	1.27	0.44**	1.21	0.78	1.47
15 to 30	0.63*	1.25	0.46	1.16	0.77	1.52
10 to 50	0.63	1.26	0.45	1.18	0.77	1.50
10 to 100	0.62**	1.27	0.43**	1.21	0.77	1.47
All	0.63	1.26	0.42**	1.21	0.80**	1.40

The protein-protein complexes in Skempi with the number of $\Delta\Delta G_{exp}$ > 0 mutations binned from 5 to 30, 10 to 30, 15 to 30, 10 to 50 and 10 to 100 were used for building the reverse mutation dataset. All: with every single forward mutation in Skempi being reversed. *p-value < 0.05 and **p-value < 0.01 compared to MutaBind2 using cutoff of "10 to 30" (Hittner2003 test).

Table S8. Performance of MutaBind2 using Modeller and FoldX to generate initial mutant structures for a reverse mutation dataset, Related to Table 1 and Figure 2.

Training/Test set	**Model**	**All mutations**			$\Delta\Delta G_{exp} \geq 0$		$\Delta\Delta G_{exp} < 0$	
		R	**RMSE**	**Slope**	**R**	**RMSE**	**R**	**RMSE**
Modeller								
Test: S1748	MutaBind2	0.63	1.25	0.83	0.45	1.17	0.77	1.52
S4191/S4191	MutaBind2	0.82	1.19	1.09	0.72	1.13	0.72	1.28
	MutaBind2 CV4	0.76	1.34	1.11	0.61	1.31	0.67	1.39
	MutaBind2 CV5	0.69	1.50	1.18	0.54	1.41	0.47	1.65
Test: S487	MutaBind2	0.41	1.25	0.59	0.39	1.20	-	1.52
Test: S877	MutaBind2	0.55	1.37	0.97	0.56	1.34	-	1.48
S4191/S3310	MutaBind2	0.76	1.16	1.07	0.72	1.13	0.74	1.25
FoldX								
Test: S1748	MutaBind2	0.62	1.27	0.84	0.46	1.15	0.73	1.60
S4191/S4191	MutaBind2	0.82	1.18	1.09	0.72	1.13	0.73	1.26
	MutaBind2 CV4	0.76	1.34	1.11	0.60	1.31	0.67	1.38
	MutaBind2 CV5	0.69	1.49	1.17	0.54	1.40	0.47	1.64
Test: S487	MutaBind2	0.43	1.23	0.61	0.42	1.17	-	1.56
Test: S877	MutaBind2	0.55	1.37	0.96	0.56	1.34	-	1.48
S4191/S3310	MutaBind2	0.75	1.17	1.08	0.72	1.13	0.70	1.31

Table S9. Performance of MutaBind2 for different types of multiple mutations, Related to Table 1 and Figure 2**.**

Type	**MutaBind2(CV4)**		
	# of mutations (# of complexes)	**R**	**RMSE**
All mutations	1707(120)	0.74	2.13
Double mutations	881(99)	0.81	2.22
Triple or higher number of mutations	826(75)	0.62	2.03
Mutations on one chain	853(105)	0.63	2.09
Mutations on multiple chains	854(43)	0.81	2.16
Double mutations on one chain	347(82)	0.66	2.04
Double mutations on multiple chains	534(31)	0.85	2.32
Triple or higher number of mutations on one chain	506(66)	0.61	2.13
Triple or higher number of mutations on multiple chains	320(25)	0.65	1.86

Table S10. Performance of MutaBind2 parameterized on different datasets where mutations with multiple experimental measurements of $\Delta\Delta G_{exp}$ were processed using different ways, Related to Table 1, Table 2 and Figure 2.

The leave-one-complex-out validation results							
Training/Test	All mutations			$\Delta\Delta G_{exp} \geq 0$		$\Delta\Delta G_{exp} < 0$	
	R	RMSE	Slope	R	RMSE	R	RMSE
S4191/S4191 (Std < 1.0)	0.76	1.34	1.11	0.61	1.31	0.67	1.39
S4944/S4944 (All values)	0.76	1.34	1.12	0.61	1.31	0.67	1.38
S4090/S4090 (Std ≤ 0.4)	0.76	1.34	1.11	0.61	1.31	0.67	1.39
S4183/S4183 (Diff < 2)	0.76	1.34	1.11	0.61	1.31	0.67	1.39

No significant difference between MutaBind2 trained and tested on S4191 and other test sets.

In the dataset of S3310, there are 408 mutations with multiple experimental measurements of binding affinity changes and their standard deviations are all less than 1 kcal mol^{-1} (The distribution of standard deviation is shown in Figure S1a). S4191: the average values were used for these 408 mutations; S4944: using all experimental measurements of $\Delta\Delta G_{exp}$ for these 408 mutations; S4090: only mutations with standard deviations with less than or equal to 0.4 kcal mol^{-1} are included in the training set, and the average value was used for these cases; S4183: only mutations with the difference between maximal and minimal $\Delta\Delta G_{exp}$ values of less than 2 kcal mol^{-1} (the cutoff was used by mCSM-PPI2) are included in the training set, and the average value was used for these cases.

Test set	Training set	R	RMSE
S487	S4191	0.41	1.25
	S4944	0.41	1.24
	S4090	0.41	1.25
	S4183	0.42	1.25
S877	S4191	0.55	1.37
	S4944	0.55	1.37
	S4090	0.55	1.37
	S4183	0.54*	1.38

*p-value < 0.05 compared to MutaBind2 trained and tested on S4191 (Hittner2003 test).

For testing on S487 set, MutaBind2 was retrained after removing S487 from the training dataset.

Table S11. The performance for MutaBind2 trained and tested on the dataset including 34 multiple mutations with more than 10 mutations using leave-one-complex-out validation, Related to Table 1 and Figure 2.

Composition of multiple mutations	**# of multiple mutations**	**R**	**RMSE**
2	881	0.79	2.27
3-5	618	0.59	2.07
6-10	208	0.74	1.92
10+	34	-	4.59

All presented values of correlation coefficients are statistically significantly different from zero (p-value << 0.01).

Transparent Methods

Experimental datasets of mutations used for training

The training dataset is compiled from the most recent SKEMPI2.0 database (Jankauskaite et al., 2019), which includes experimentally measured values of dissociation constants for wild-type and mutant proteins with the available crystal structures. Changes in binding affinity are also provided in SKEMPI2.0 and calculated as $\Delta G = RTln(K_D)$. We applied the following criteria to the SKEMPI2.0 data set by removing the following complexes and mutations: (a) complexes with modified residues at the protein-protein binding interface; (b) complexes containing a chain of less than 20 residues long; (c) mutations with mutated sites having missing coordinates; (d) changes in affinity measured by an 'unusual method' as defined in SKEMPI2.0; (e) mutations on metal coordination sites; (f) mutations without binding affinity experimental values; and (g) entries with ten or more multiple mutations (Figure S1). There are 408 mutations with multiple experimental measurements of changes in binding affinity and their standard deviations are all less than 1.0 kcal mol^{-1} (Figure S1a), and the average value was used for these cases. Three additional ways to process these cases were tried but the performance did not change (Table S10). As the number of multiple mutations with more than 10 mutations is small and prediction accuracy for these multiple mutations is low (Table S11), the upper limit of 10 mutations was used in the study. As a result, 3,310 single mutations from 265 wild-type protein-protein complexes (it will be referred to as S3310) and 1,337 multiple mutations from 120 wild-type protein-protein complexes (it will be referred to as M1337) were retained (Table S1 and Figure S2). *Multiple mutations* correspond to cases where several mutations are introduced on one or several chains of a protein complex simultaneously.

The Gibbs free energy ($\Delta\Delta G$) of a system can be represented as a thermodynamic state function where the absolute values of $\Delta\Delta G$ for a *forward mutation* ($\Delta\Delta G_{wt\rightarrow mut}$) and $\Delta\Delta G$ for the *reverse mutation* ($\Delta\Delta G_{mut\rightarrow wt}$) should be approximately equal to each other. In order to prepare a more balanced training dataset, we augmented the existing mutations increasing binding affinity from the forward mutation sets with the modelled reverse mutations (see Table S1). In order to balance the prediction accuracy for both types of mutations: decreasing and increasing binding affinity, we used protein complexes with the number of experimentally characterized mutations from 10 to 30 and 10 to 50 to build the single and multiple reverse mutation dataset respectively. The performance is shown in Table S7. Therefore, the final training set including both forward and reverse mutations comprised 4,191 single mutations from 265 wild-type protein complexes (it will be referred to as S4191) and 1,707 multiple mutations from 120 wild-type protein complexes (it will be referred to as M1707), respectively (Table S1).

Structure optimization protocol

For the forward mutation datasets S3310 and M1337 ($\Delta\Delta G_{wt\rightarrow mut}$), the structure optimization protocol was the same as the one used in MutaBind (the flowchart for the structure optimization protocol is shown in Figure S3). Namely, we used the BuildModel module of FoldX (Guerois et al., 2002) to introduce single or multiple point mutations on the wild-type crystal structure obtained from the Protein Data Bank (PDB) (Berman et al., 2000). Next we added missing heavy side-chain and hydrogen atoms via the VMD program (Humphrey et al., 1996) using the topology parameters of the CHARMM36 force field (MacKerell et al., 1998). After that we performed a 100-step energy minimization in the gas phase for both wild-type and mutant complex structures applying harmonic restraints with the force constant of 5 kcal mol^{-1} Å^{-2} on the backbone atoms of all residues. The energy minimization was carried out by NAMD program version 2.9 (Phillips et al., 2005) using the force field CHARMM36 (MacKerell et al., 1998). A 12 Å cutoff distance for nonbonded interactions was applied to the systems. Lengths of hydrogen-containing bonds were constrained by the SHAKE algorithm (Hoover, 1985).

For the reverse mutation datasets, we modeled the mutant structures with the Modeller software (Sali and Blundell, 1993) using wild-type crystal structures as the templates (Table S8). To minimize the error introduced by structural modelling, only the mutated protein chain was modeled for single mutations, and for multiple mutations on multiple protein chains, the whole complex was modelled. The structural model was discarded if the root-mean-square deviation of all aligned C_α atoms between any of the modelled chains and the template was larger than 2 Å. Then the RepairPDB module was applied to further optimize the structure and mutations were introduced using the BuildModel module from FoldX. After that a 1000-step energy minimization in the gas phase was carried out for both wild-type and mutants using harmonic restraints (with the force constant of 5 kcal mol^{-1} Å^{-2}) applied on backbone atoms of all residues using NAMD. Minimization was performed for the whole protein complex.

Calculating changes in binding affinity

The scoring function of MutaBind2 includes seven distinct terms for single and multiple mutations, it is parameterized using the S4191 and M1707 datasets (Table S1), respectively. The terms that contribute significantly to the quality of the MutaBind2 single and multiple mutation models are shown in Table S2 and described below.

The six terms of the scoring function described below are common for both single and multiple mutation models.

- $\Delta\Delta E_{vdw}$ is the change of van der Waals interaction energy upon a single or multiple mutation(s) ($\Delta\Delta E_{vdw} = \Delta E_{vdw}^{mut} - \Delta E_{vdw}^{wt}$). ΔE_{vdw} is calculated as a difference between van der Waals energies of a complex and each interacting partner using the ENERGY module of CHARMM (Brooks et al., 1983). The minimized structure of the wild-type or mutant complex structure was used for the calculation.

- $\Delta\Delta G_{solv}$ approximates the change of polar solvation energy upon mutation(s) ($\Delta\Delta G_{solv} = \Delta G_{solv}^{mut} - \Delta G_{solv}^{wt}$), ΔG_{solv} is obtained from numerically solving the Poisson-Boltzmann (PB) equation with the PBEQ module (Im et al., 1998) of the CHARMM program using the minimized structure of the wild-type or mutant complex. For the PB calculation, dielectric constants $\varepsilon = 2$ for the protein interior and $\varepsilon = 80$ for the exterior aqueous environment were used.
- $\Delta\Delta G_{fold}$ is the change in stability of the protein complex upon mutation(s) ($\Delta\Delta G_{fold} = \Delta G_{fold}^{mut} - \Delta G_{fold}^{wt}$) where each term is defined as the unfolding free energy of the mutant and wild-type protein complexes. It is calculated with the BuildModel module from the FoldX software (Guerois et al., 2002) which uses an empirical force field. This term may account for those cases where mutated proteins are unfolded in unbound states and can only fold upon binding to its partner.
- SA_{part}^{wt} and SA_{com}^{wt} are solvent accessible surface areas of the mutated residues in the wild type unbound partner and complex structure respectively. These terms are calculated by the DSSP program (Joosten et al., 2011) using the crystal structure of the wild-type complex. For multiple mutations this term is calculated as a sum of the solvent accessible surface areas of all mutated residues.
- CS is the change of evolutionary conservation of a mutated site upon introducing mutations calculated using the PROVEAN program (Choi et al., 2012). This is used to account for the fact that a site can be evolutionary conserved because it is important for interactions with other proteins and any change in this site may affect its function in a detrimental way. For multiple mutations this term is calculated by summing up CS for all mutations.

A scoring function for single mutations included an additional term, N_{cont}^{wt}, representing the number of interactive residues between one partner where a mutation was introduced and another partner in a wild type structure. If any heavy atom of a residue in one partner was located within 10 Å from any heavy atom of another partner, we defined this residue as an interactive residue. A scoring function for multiple mutations included an additional term ΔE_{vdw}^{wt} calculated as a difference between van der Waals energies of a complex and each interacting partner for the wild-type structure, as described above.

MutaBind2 predictive models were built using the random forest (RF) regression algorithm implemented in the R package "randomForest" using Breiman's random forest algorithm (Breiman, 2001). Hyperparameter optimization in a balanced "CV2" cross-validation (see the section below) suggested that the number of trees "ntree" parameter should be set to 500 and the number of features/terms randomly sampled as candidates for splitting at each node ("mtry") should be set to 2. Feature importance in RF models is shown in Supplementary Table 2 and all features listed above contribute significantly to the quality of the models. The performance of MutaBind2 trained on S4191 and M1707 sets is shown in Table S3 and Figure S4c. The Pearson correlation coefficient between experimental and calculated changes in binding affinity is R = 0.82 and the corresponding root-mean-square error (RMSE) is 1.19 kcal mol^{-1} for single mutations and R = 0.87 and the RMSE is 1.61 kcal mol^{-1} for multiple mutations. We also tested the performance of other algorithms, including Support Vector Machine (SVM) and eXtreme Gradient Boosting (XGBoost), however, the random forest regression algorithm shows the best performance (Table S4).

MutaBind2 calculations take several minutes for a single mutation in a protein complex of about 350 residues, and require less than a minute for each additional mutation introduced in the same complex and therefore require about 12 hours for calculations of one thousand mutations (Figure S10).

Five types of cross-validation (CV) procedures

We performed five types of cross-validation. In the "CV1" cross-validation, 80% of all mutations from S4191 or M1707 set were randomly selected to train the model and the remaining 20% of the mutations were used for testing; we repeated the procedure 100 times. For "CV2" cross-validation, 50% of the mutations were randomly chosen for training and the remaining mutations for testing, also repeated 100 times. As shown in Figure S2, the distribution of the number of mutations per protein is not uniform, so to take this bias into account, we performed the third type of cross-validation ("CV3"). First, we randomly sampled up to ten mutations per protein complex from S4191 and M1707, the procedure was repeated 10 times and yielded ten subsets. Then 80 percent of the mutations were randomly selected from each subset for training and the rest for testing, repeated 10 times.

We also performed the "CV4" cross-validation by leaving one complex and its mutations out as a test set and using the rest of the complexes/mutations to train the model, repeating this process for each protein complex. In addition, a "CV5" cross-validation accounted for similarities between binding sites of different complexes (the definition of similar binding sites is taken from (Jankauskaite et al., 2019; Moal and Fernandez-Recio, 2012)). Namely, we used all complexes and corresponding mutations from one cluster/type of binding site for testing and trained the model on the rest of the complexes/mutations, repeated for each type of binding site. During the cross-validation procedures, forward and reverse mutations were kept in the same set, either training or testing.

Assessment of quality of classification

One way to evaluate the performance of MutaBind2 is to assess the quality of classification of mutations into mutations with large amplitudes of their effects on binding affinity: highly decreasing ($\Delta\Delta G \geq 1.5$ kcal mol^{-1}) and highly increasing ($\Delta\Delta G \leq -1.5$ kcal mol^{-1}). The explanation is provided in Figure S6c and Figure S6d.

Prediction performance was measured using area under the ROC curve (AUC), accuracy, precision, sensitivity, specificity, negative predictive value (NPV) and Matthews correlation coefficient (MCC). Positives and negatives were defined as those mutations with predicted $\Delta\Delta G$ values within or outside the range specified above for experimental $\Delta\Delta G$ values. The accuracy was defined as a percentage of correctly classified mutations (true positives, TP, and true negatives, TN) out of the total number of mutations (TP + TN)/(TP + TN + FP + FN), where FN are false negatives, and FP are false positives. Sensitivity was defined as TP/(TP + FN), specificity was calculated as TN/(TN + FP) (false negatives, FN and false positives, FP). Additionally, in order to account for imbalances in the labeled dataset, the quality of the predictions was described by the Matthews correlation coefficient (MCC), a performance measure which is known to be more robust on unbalanced datasets:

$$\mathrm{MCC} = \frac{TP * TN - \mathrm{FP} * \mathrm{FN}}{\sqrt{(TP + FP)(TP + FN)(TN + FP)(TN + FN)}}$$

Supplemental References

Berman HM, Westbrook J, Feng Z, Gilliland G, Bhat TN, Weissig H, Shindyalov IN and Bourne PE. (2000). The Protein Data Bank. Nucleic Acids Research 28, 235-242.

Breiman L. (2001). Random Forests. Machine Learning 45, 5-32.

Brooks BR, Bruccoleri RE, Olafson BD, States DJ, Swaminathan S and Karplus M. (1983). Charmm - a Program for Macromolecular Energy, Minimization, and Dynamics Calculations. Journal of Computational Chemistry 4, 187-217.

Choi Y, Sims GE, Murphy S, Miller JR and Chan AP. (2012). Predicting the functional effect of amino acid substitutions and indels. Plos One 7, e46688.

DeLong ER, DeLong Dm Fau - Clarke-Pearson DL and Clarke-Pearson DL. Comparing the areas under two or more correlated receiver operating characteristic curves: a nonparametric approach. Biometrics 44, 837-845.

Diedenhofen B and Musch J. (2015). cocor: a comprehensive solution for the statistical comparison of correlations. PLoS One 10, e0121945.

Fragoza R, Das J, Wierbowski SD, Liang J, Tran TN, Liang S, Beltran JF, Rivera-Erick CA, Ye K, Wang TY, et al. (2019). Extensive disruption of protein interactions by genetic variants across the allele frequency spectrum in human populations. Nat Commun 10, 4141.

Guerois R, Nielsen JE and Serrano L. (2002). Predicting changes in the stability of proteins and protein complexes: a study of more than 1000 mutations. Journal Of Molecular Biology 320, 369-387.

Hittner JB, May K and Silver NC. (2003). A Monte Carlo evaluation of tests for comparing dependent correlations. J Gen Psychol 130, 149-168.

Hoover WG. (1985). Canonical dynamics: Equilibrium phase-space distributions. Phys Rev A 31, 1695-1697.

Humphrey W, Dalke A and Schulten K. (1996). VMD: visual molecular dynamics. J Mol Graph 14, 33-38, 27-38.

Im W, Beglov D and Roux B. (1998). Continuum Solvation Model: computation of electrostatic forces from numerical solutions to the Poisson-Boltzmann equation. Computer Physics Communications 111, 59-75.

Jankauskaite J, Jimenez-Garcia B, Dapkunas J, Fernandez-Recio J and Moal IH. (2019). SKEMPI 2.0: an updated benchmark of changes in protein-protein binding energy, kinetics and thermodynamics upon mutation. Bioinformatics 35, 462-469.

Joosten RP, te Beek TA, Krieger E, Hekkelman ML, Hooft RW, Schneider R, Sander C and Vriend G. (2011). A series of PDB related databases for everyday needs. Nucleic Acids Research 39, D411-419.

MacKerell AD, Bashford D, Bellott M, Dunbrack RL, Evanseck JD, Field MJ, Fischer S, Gao J, Guo H, Ha S, et al. (1998). All-atom empirical potential for molecular modeling and dynamics studies of proteins. J Phys Chem B 102, 3586-3616.

Moal IH and Fernandez-Recio J. (2012). SKEMPI: a Structural Kinetic and Energetic database of Mutant Protein Interactions and its use in empirical models. Bioinformatics 28, 2600-2607.

Phillips JC, Braun R, Wang W, Gumbart J, Tajkhorshid E, Villa E, Chipot C, Skeel RD, Kale L and Schulten K. (2005). Scalable molecular dynamics with NAMD. Journal of Computational Chemistry 26, 1781-1802.

Rodrigues CHM, Myung Y, Pires DEV and Ascher DB. (2019). mCSM-PPI2: predicting the effects of mutations on protein–protein interactions. Nucleic Acids Research 47, W338-W344.

Sali A and Blundell TL. (1993). Comparative protein modelling by satisfaction of spatial restraints. Journal Of Molecular Biology 234, 779-815.